A new method for analyzing the local structures of disordered systems

To cite this article: Z. A. Tian *et al* 2011 *EPL* **96** 36001

View the article online for updates and enhancements.

A new method for analyzing the local structures of disordered systems

Z. A. Tian[1,2], R. S. Liu[1], K. J. Dong[2] and A. B. Yu[2(a)]

[1] *School of Physics and Microelectronic Science, Hunan University - Changsha 410082, China*
[2] *School of Materials Science and Engineering, University of New South Wales - Sydney, NSW 2052, Australia*

Abstract – We present a novel method to identify local structures in disordered systems according to topological criteria. Its effectiveness is demonstrated in the analysis of the atomic structures in the rapid cooling of silver liquid. The method is parameter free and scale independent, and can generally be used for structural analysis of amorphous systems involving atoms or particles at different length scales.

Structures are very important in determining materials properties and functions. In the past, the determination of atomic structures was notoriously difficult for many materials which often lack long-range periodicity, *e.g.*, metallic and covalent glasses [1,2]. With the rapid development of experimental and/or simulation technologies, it is now possible to obtain enormous three-dimensional (3D) coordinates of atoms or particles [3–7]. However, it is still very challenging to develop an effective method that can quantify the structure of such a system based on the 3D coordinates.

Many techniques have been developed in the past to analyze the local structures, but there are problems in discriminating local structures. The most commonly used technique is the Voronoi tessellation [8]. In fact, since the work of Bernal [9] and Finney [10], it has been widely accepted as a powerful tool to study the structure of disordered systems. The structural information revealed by this method is however limited to neighbor atoms. Many similar but different local structures cannot be distinguished simply from the topological and metric properties of a Voronoi cell [11]. Similarly, a Delaunay cell (the dual of Voronoi tessellation) [12] as a tetrahedron composed of only 4 atoms is too simplistic to describe the complicated arrangements which may involve many atoms in a representative geometric cluster. This remark is largely also applicable to other methods focusing on simple geometric units or cells.

Various methods have been proposed in the past two decades to overcome this limitation. According to the size of local structures concerned, they can be classified in two categories: pair-analysis such as the (Honeycutt-Anderson) HA-pair [13,14], and CNA (Common Neighbor Analysis) [15], and cluster-analysis such as the BCA (where a local structure composed of a central atom and its neighbors within a spherical region of a pre-set radius is defined as a basic cluster) [11,16] and SPR-PG (a topological technique combining the Shortest-Path Ring and Planar Graph) [17,18]. These methods have the capability to distinguish different structures to various degrees of success, and indeed are more and more widely used to study the icosahedral ordering in liquids and glasses [11,14], the local structure in nanoparticles [18], and the structural evolution of particles [15] and various atomic systems [19]. However, the results of both pair- and cluster-analysis are very sensitive to a pre-set parameter, namely the cutoff distance r_c less than which two atoms are neighbors or bonded, when a system is not a perfect crystal [20–22]. The fact that structural outcomes vary with r_c will result in an uncertainty in structural quantification. A similar problem can also be found in calculating other parameters such as ADF (Angle Distribution Function) [23] and BOO (Bond Orientation Order) [24] parameters which detect the local and/or global symmetry of a system.

This letter presents a new method of overcoming these difficulties with topological criteria. First, the fundamental concepts of this new methodology are defined. Then its
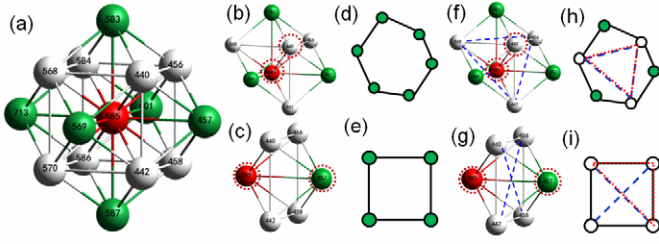

(a)E-mail: a.yu@unsw.edu.au

Fig. 1: (Color online) Topological analysis of a bcc cluster: a bcc LSC (a); two standard center-neighbor-subclusters ((b) and (c)), and the topologies of their common-near-neighbors ((d) and (e)); similarly, (f)–(i) show two non-standard center-neighbor-subclusters which include multi-bonded-points and common-neighbor-subrings. Balls circled by dotted lines are root-pairs, and open circles are multi-bonded-points.

implementation is described. Finally, a case study about the microstructural evolution in the rapid cooling of liquid silver is presented to demonstrate the advantage of this method.

The new method is developed based on a number of important concepts at three hierarchical levels: cluster, center-neighbor-subcluster, and common-near-neighbor. As illustrated in fig. 1(a), a structure composed of a center atom and its near neighbors in a spherical region of radius r is defined as a cluster with radius r. Any two points in a cluster are near neighbors or bonded if they depart less than r. A center-neighbor-subcluster in a cluster is defined by: 1) a root-pair composed of the center and one of its neighbors, 2) the common-near-neighbors shared by the root-pair, and 3) the bonds between the common-near-neighbors (see figs. 1(b) and (c)). At the common-near-neighbor level, a multi-bonded-point is a common-near-neighbor where more than two bonds between common-near-neighbors meet together, and a common-neighbor-subring is a closed chain in which part (not all) of common-near-neighbors are bonded one by one. A center-neighbor-subcluster without multi-bonded-point or common-neighbor-subring is a standard center-neighbor-subcluster, otherwise is a non-standard center-neighbor-subcluster. Clusters without non-standard center-neighbor-subcluster are standard clusters, and among all standard clusters around an atom the largest one is defined as the Largest Standard Cluster (LSC).

A center-neighbor-subcluster can be systematically classified by a set of four indices, $ijkl$. If the root-pair is bonded, i is 1; otherwise it is 2. j is the number of common-near-neighbors. k equals the number of all bonds between common-near-neighbors. The last index l is the number of bonds in the longest continuous chain formed by the k bonds. We call a set of four-indices a CNS-index. It is noticeable that the last index is different from that of the HA-index [13].

For the example shown in fig. 1, given the nearest distance between atoms is a in a body-centered cubic

(bcc) crystal, a bcc cluster (see fig. 1(a)) composed of 8 first neighbors and 6 second neighbors can be identified when its radius is within $(2a/\sqrt{3}, \sqrt{6}a/2)$. There are only two types of center-neighbor-subclusters in such a bcc cluster. The first one is a 1666 center-neighbor-subcluster (fig. 1(b), abbreviated as S1666) where: 1) the center and one of the first neighbors comprise the bonded root-pair, 2) 6 common-near-neighbors are shared by the root-pair, and 3) 6 bonds between all common-near-neighbors form the largest and unique ring (see fig. 1(d)). And the second center-neighbor-subcluster is a S1444 (figs. 1(c) and (e)). No common-neighbor-subring or multi-bonded-point exists in these two center-neighbor-subclusters, both of these are thus standard center-neighbor-subclusters, and the bcc cluster shown in fig. 1(a) is hence a standard cluster. When $r > \sqrt{6}a/2$, many third neighbors will be involved in a bcc cluster, and the center-neighbor-subclusters will become very complicated. The two center-neighbor-subclusters shown in figs. 1(b) and (c) will be changed to those as shown in figs. 1(f) and (g) (all third neighbors are not shown for simplicity), respectively. The appearance of the bonds plotted by dashed lines will result in multi-bonded-points (open circles in figs. 1(h) and (i)) and common-neighbor-subrings. Both center-neighbor-subclusters shown in figs. 1(f) and (g) are thus non-standard center-neighbor-subclusters, and the clusters including third neighbors are not standard clusters. In other words, the cluster shown in fig. 1(a) is the unique bcc LSC.

Based on the above concepts, the unique LSC around each atom in a considered system can be identified by means of the following steps:

1) Set an initial searching distance r_s and the sequence n of atoms as $1(n = 1)$.

2) Construct the initial temporary cluster around atom n by searching all temporary neighbors within a spherical region of radius r_s.

3) Check all center-neighbor-subclusters in the initial temporary cluster. If no non-standard center-neighbor-subcluster is found, then turn to step 4), otherwise 5).

4) Set a larger r_s, and turn to step 2).

5) Remove the longest bond from the current temporary cluster which includes at least one non-standard center-neighbor-subcluster. If a bond between the center and a temporary neighbor is removed, then the temporary neighbor is removed from the current temporary cluster.

6) Check all remaining center-neighbor-subclusters in the current temporary cluster. If no non-standard center-neighbor-subcluster is found (it is a LSC), turn to step 7), otherwise 5).

7) Quantify the type of the standard cluster around atom n, and increase the sequence as $n = n + 1$; if $n < N$ (N is the total number of atoms), return to step 2), otherwise end.
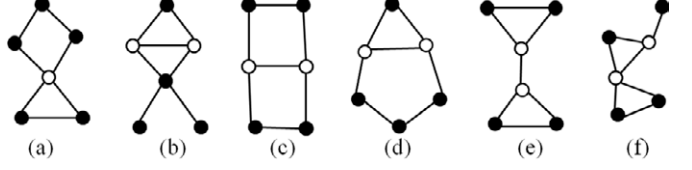
We call this computational rule a reduction algorithm, because the size of the initial temporary cluster with non-standard center-neighbor-subclusters is always larger than the final LSC. Correspondingly, the new method is known as the Largest Standard Cluster Analysis (LSCA).

In the previous methods, a constant r_c is used. This is problematic because different local structures cannot always be identified by a single r_c [13,21]. This problem does not exist in LSCA, because firstly, steps 2)–4) ensure that all initial local structures are in an identical state where there is at least one non-standard center-neighbor-subcluster; and secondly by gradually decreasing r_s, the radius r of the final LSC can vary to take into account the unique local structure of each atom. In this way, all LSCs can be determined with a varying r_s. However, differently from the previous methods [11,13–18], r_s only acts as an intermediate parameter in this searching process. Therefore, the new method is parameter free and scale independent.

To define standard clusters, we introduce a compact nomenclature as follows. Each standard cluster is characterized by a set of index-pairs. An index-pair composed of a CNS-index and an integer, which, respectively, represent the type and the total of a kind of center-neighbor-subclusters in a standard cluster. For example, the bcc LSC shown in fig. 1(a) is denoted as (1444-6, 1666-8). Similarly, face-centered cubic (fcc), hexagonal close-packed (hcp), icosahedral, and truncated decahedral LSCs are (1421-12), (1421-6, 1422-6), (1555-12), and (1422-10, 1555-2), respectively.

Both LSCA and the new nomenclature are more general than the previous ones. The structures identified by the HA-pair and CNA [13–15,20] do not belong to a particular atom, thus they cannot describe the local feature around a specified atom. In fact, the nomenclature of the previous cluster analysis methods is not systematic and only part of the clusters can be denoted. For example, CTIM (Cluster Type Index Method, which is used by BCA) can only denote those composed of five kinds of center-neighbor-subclusters (S1444, S1555, S1666, S1421, and S1422) [16]. Many important clusters, *e.g.*, those including S1433 and S1544, cannot be denoted. LSCA can identify all LSCs and the new nomenclature can label them irrespective of their locations, sizes, and shapes. Atoms can then be classified completely by the type of LSC around them. For example, the centers of fcc, hcp, and bcc LSCs are known as fcc, hcp, and bcc atoms, respectively. As a result of the complete classification, with the help of 3D visualization, many global properties such as the complex phase distribution [16], and the multi-fold symmetry of nanoclusters [25] can be further studied.

Fig. 2: Six of the possible topologies for the common-near-neighbors in the HA-pair 1671. Open circles are multi-bonded-points.

To demonstrate the applicability of this LSCA method, we have chosen a rapid cooling process of liquid silver as a case study, where the structural evolution in phase transition is closely related to materials function. The structural data for the present analysis are generated by means of molecular-dynamics simulation, as reported elsewhere [19]. However, we enlarge the system from 500 to 50,000 atoms here to generate more reliable data and focus on the liquid-solid transition at the cooling rate of 5×10^{11} K/s. Ostwald [26] proposed the rule of stages: an unstable system could transform into a transient state the formation of which is attained by the smallest loss of free energy before finally reaching a stable state. This rule was confirmed experimentally by Chung and colleagues for $LiFePO_4$ [27], but it is a long-standing problem if metal melt complies with this rule. Studies on fcc metals are somewhat contradictory on the availability of bcc lattice during the liquid-crystal transition [28,29]. It would also be very useful to check whether the escalation of bcc clusters is earlier than fcc/hcp ones in a rapid cooling process.

Here the advantage of the proposed LSCA method is demonstrated mainly through the comparison with two representative "old" methods: BCA [16] and BOO [24]. Among all basic clusters determined by a pre-set r_c, only standard clusters are quantified by BCA. Simply discarded are those clusters containing non-standard center-neighbor-subclusters which are inevitable for such a single r_c, otherwise the appearance of multi-bonded-points and common-neighbor-subrings will generate too many kinds of non-standard center-neighbor-subclusters and hence too many clusters to evaluate local structures effectively. For example, there are many possible topologies for the HA-pair 1671 [30], and six of them are shown in fig. 2. BCA and BOO can assume different r_c. Here a series of r_c obtained from the first minimum of RDFs (assigned as r_c^{RDF}, see fig. 3), and three invariant r_c^i (0.3644, 0.3783, and 0.3922 nm) which are in the close vicinity of r_c^{RDF} are used to analyze the structural evolution in the rapid cooling process. The results are shown in fig. 4 for r_c^{RDF} and fig. 5 for r_c^i.

The weakness of BCA and BOO can be reflected by the following facts: a pre-set r_c is necessary to effect structural analysis, and it is usually very difficult to choose a proper r_c. In fact, because the results are very sensitive to the pre-set r_c, such a proper r_c may not exist. As shown in
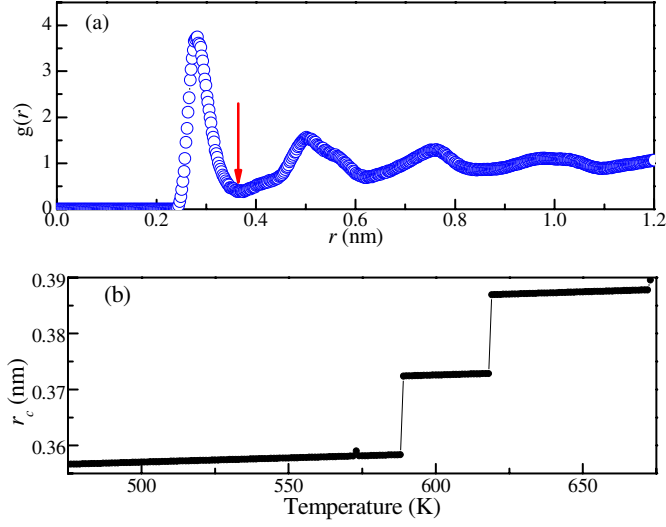
Fig. 3: (Color online) RDF at temperature $T = 600$ K (a), and r_c at different temperatures (b), where r_c is obtained from the first minimum of a RDF as indicated in (a).
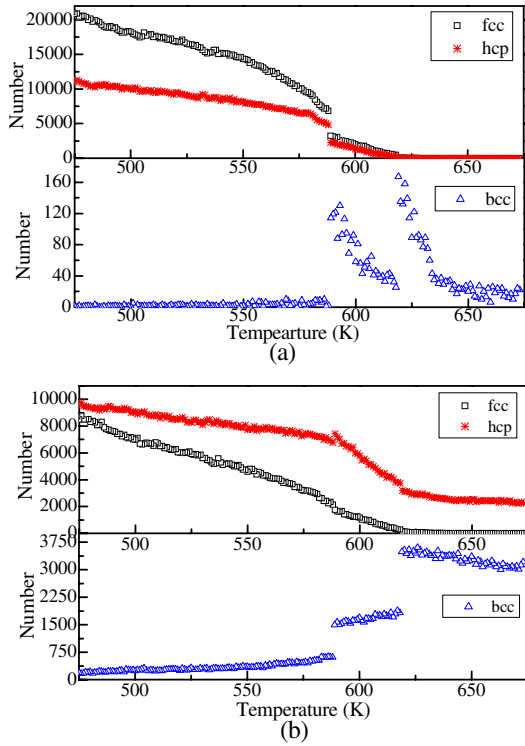

Fig. 4: (Color online) N-T plots (the number of clusters *vs.* temperature), respectively obtained by BCA (a) and BOO (b).

fig. 4, corresponding to two down-jumps of r_c^{RDF} at 620 and 590 K, not only does the number of considered clusters have two up- or down-jumps, but also the evolution of numbers of bcc clusters has two oddly increasing-vanishing recycles (fig. 4(a)) or large down-jumps (fig. 4(b)) in ranges of (645, 620) K and (620, 590) K. Note that for both BCA and BOO, no up- and down-jumps can be found for a constant r_c as shown in fig. 5. Thus, the two
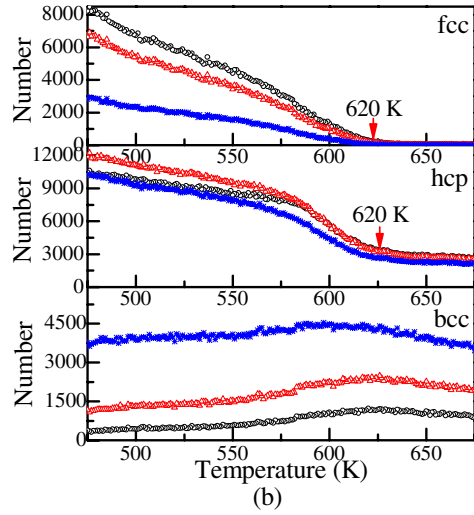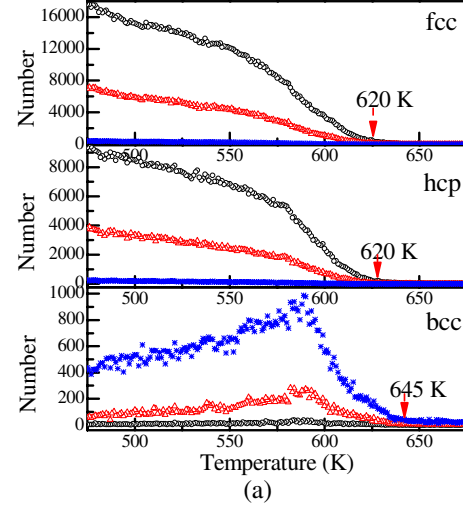

Fig. 5: (Color online) N-T plots respectively obtained by BCA (a) and BOO (b) at three different r_c (∘, 0.3644 nm; Δ, 0.3783 nm; ∗, 0.3922 nm).

jumps of cluster numbers must result from the varying $r_c = r_c^{RDF}$. It can be observed from fig. 5 that a small difference ($< 7.5\% \approx \frac{0.3922 - 0.3644}{(0.3922 + 0.3644)/2}$) among r_c^i results in a large discrepancy in the number of fcc, hcp or bcc clusters. Consequently, useful information of a considered system may have to be obtained by trial and error. For example, three critical temperatures of 645, 620, and 590 K can be obtained by BCA through r_c^{RDF} (fig. 4(a)), but they are highly questionable before being validated by three constant r_c^i (fig. 5(a)); only two critical points of 620 and 590 K can be identified by BOO (see figs. 4(b) and 5(b)). Moreover, some critical structures may be missing if r_c used is not appropriate. For example, the number of bcc clusters obtained both by BCA and BOO is negligible compared to that of fcc/hcp ones when r_c is 0.3644 or 0.3783 nm (fig. 5). Because the results of the present case are so sensitive to the selection of r_c, it is difficult to derive conclusions from the BCA or BOO results.
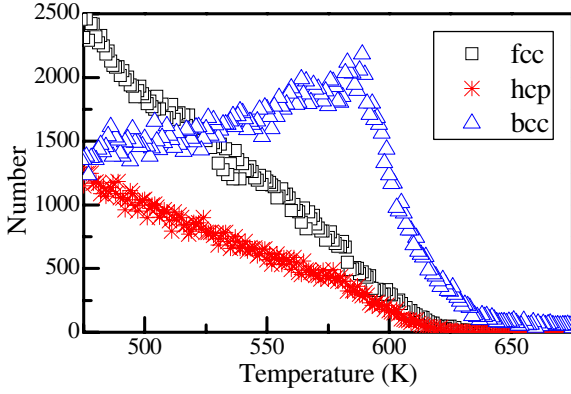
Fig. 6: (Color online) The N-T plots for fcc, hcp, and bcc clusters obtained by LSCA.

Fig. 7: (Color online) The number distribution at 590 K of three crystalline clusters based on different r_c.

The above problems associated with BCA and BOO can all be overcome by the use of the proposed LSCA. The parameter-free advantage leads to unique and definitive results (fig. 6). In particular, the meta-stable bcc structures, which are believed to be the most important precursor in silver crystallization [19,28,29], can be identified. In fact, the number of bcc LSCs is more than the sum of fcc/hcp ones within $(645, 550)$ K. This is consistent with the previous study [19] and Ostwald's rule of stages [26]. However, BCA and BOO are difficult to determine the role of clusters in the phase transition, because with the increase of r_c^i, the number of bcc clusters increases while that of fcc/hcp clusters decreases.

Why are the results from LSCA more reliable than those from the "old" methods such as BCA and BOO? Fundamentally, a single r_c is unreasonable for different clusters. Provided atoms are uniform spheres with diameter a and are closely in contact, to identify fcc/hcp clusters, the requirement for a cut-off distance is just $r_c^{fcc} > a$; while for bcc ones, $r_c^{bcc} > 1.1547a$. Therefore, no matter how to choose a single r_c for such a disordered system, some kinds of clusters cannot be identified correctly by BCA or BOO. For a mixture of fcc, hcp, bcc, and other structures, r_c^{RDF} is usually very close to r_c^{fcc}. For example, for the present system at 590 K, $r_c^{RDF} \approx 0.37$ nm (fig. 3(b)), but r_c giving the maximum numbers of bcc, fcc/hcp LSCs are about 0.40 and 0.36 nm, respectively (fig. 7). Thus, with the increase of r_c^i in $(0.36, 0.40)$ nm, the number of fcc/hcp clusters obtained by BCA and BOO decreases while that of bcc ones increases. Furthermore, many spurious fcc/hcp standard clusters are easy to produce from deformed bcc and other larger LSCs by removing the farthest one or two atoms as r_c is between r_c^{fcc} and r_c^{bcc}. However, no smaller LSC can be quantified as larger bcc clusters by adding few atoms because of the inevitability of non-standard center-neighbor-subclusters. Therefore, more bcc clusters are identified by LSCA (fig. 6), while more fcc/hcp clusters are identified by BCA and BOO as r_c is in (r_c^{fcc}, r_c^{bcc}) (figs. 4 and 5). Clearly, different clusters may have different radii in disordered systems; hence it is impossible to
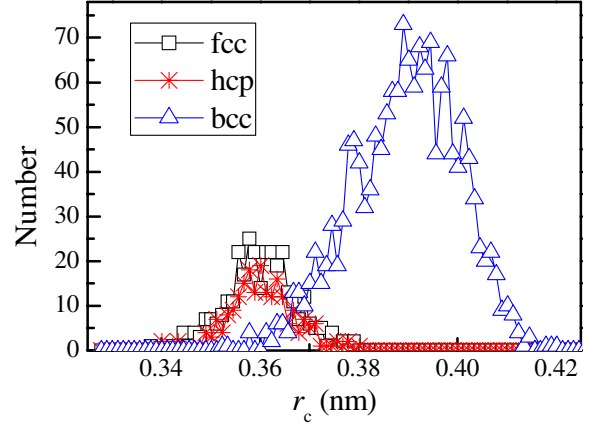
identify all different clusters using one pre-set cutoff. LSCA can overcome this problem and hence generate more reliable results.

It should be pointed out that LSCA is proposed for both ordered and disordered systems at different length scales, although the above example is somehow close to ordered systems. In fact, it has been used to analyze the packing of uniform spheres, which can provide much richer structural details about the critical states recently identified by Dong *et al.* [31]. The work will be submitted for publication soon.

In summary, we have proposed a new method, namely LSCA, to quantify the local structures in disordered systems. On the one hand, the structures identified by LSCA are similar to those by the previous methods, including, for example, the center-neighbor-subcluster identified by the HA-pair [13,14] or CNA [15], and the basic cluster defined in other techniques [11,17,18,23,24]. On the other hand, a simple but effective criterion for the unique largest cluster can be found by a reduction algorithm, so that the multi-bonded-point and common-neighbor-subring can be eliminated in LSCA. The new method can certainly be applied to all the systems dealt with by the previous approaches and provide more reliable results. It has various advantages over the previous methods: 1) it is parameter free, without the use of somewhat arbitrary r_c; 2) it has better capability to distinguish different local structures; and 3) it decreases the possible types of center-neighbor-subclusters, so that all kinds of local structures can be identified, denoted and classified completely. Moreover, LSCA offers a method to compare the geometrical property of different systems, because structures at different sizes and/or scales are identical in LSCA as long as they hold the same topology. On the other hand, this may be a weakness when the properties considered (*e.g.*, the energy of clusters) are sensitive to both topology and size; but this size effect is usually not concerned in the structural analysis of a given system. Therefore, as demonstrated by the example described above, LSCA not only overcomes the difficulties

of the previous methods, but also is more effective. Our LSCA results confirm that Ostward's rule of stages hold for metal melt, at least for silver melt. It is considered that LSCA can generally be used to analyze the structures of atomic or particle systems, leading to improved understanding about structure-property relationships.

$$* * *$$

REFERENCES

[1] BILLINGE S. J. L. and LEVIN I., *Science*, **316** (2007) 561.

[2] BYRNE C. J. and ELDRUP M., *Science*, **321** (2008) 502.

[3] JUHS P., CHERBA M., DUXBURY P. M., PUNCH W. F. and BILLINGE S. J. L., *Nature*, **440** (2006) 655.

[4] CLIFFE M. J., DOVE M. T., DRABOLD D. A. and GOODWIN A. L., *Phys. Rev. Lett.*, **104** (2010) 125501.

[5] STREITZ F. H., GLOSLI J. N. and PATEL M. V., *Phys. Rev. Lett.*, **96** (2006) 225701.

[6] BORRELL B., *Nature*, **451** (2008) 240.

[7] ZHU H. P., ZHOU Z. Y., YANG R. Y. and YU A. B., *Chem. Eng. Sci.*, **62** (2007) 3378; **63** (2008) 5728.

[8] VORONOI G. F., *J. Reine Angew. Math.*, **134** (1908) 198.

[9] BERNAL J. D., *Nature*, **183** (1959) 141.

[10] FINNEY J. L., *Proc. R. Soc. London, Ser. A*, **319** (1970) 479.

[11] QI D. W. and WANG S., *Phys. Rev. B*, **44** (1991) 884.

[12] DELAUNAY B., *Otd. Mat. Estestv. Nauk*, **7** (1934) 793.

[13] HONEYCUTT J. D. and ANDERSON H. C., *J. Phys. Chem.*, **91** (1987) 4950.

[14] JONSSON H. and ANDERSEN H. C., *Phys. Rev. Lett.*, **60** (1988) 2295.

[15] CLARKE A. S. and JONSSON H., *Phys. Rev. E*, **47** (1993) 3975.

[16] TIAN Z. A., LIU R. S., LIU H. R., ZHENG C. X., HOU Z. Y. and PENG P., *J. Non-Cryst. Solids*, **354** (2008) 3705.

[17] FRANZBLAU D. S., *Phys. Rev. B*, **44** (1991) 4925.

[18] YU H. C., ROBERT J. R., IAN K. S., O'MALLEY B. and SALVY P. R., *J. Chem. Phys.*, **125** (2006) 114703.

[19] TIAN Z. A., LIU R. S., ZHENG C. X., LIU H. R., HOU Z. Y. and PENG P., *J. Phys. Chem. A*, **112** (2008) 12326.

[20] BLAISTEN-BAROJAS E., *Kinam*, **6A** (1984) 71.

[21] YU D. Q., CHEN M. and HAN X., *J., Phys. Rev. E*, **72** (2005) 051202.

[22] GANESH P. and WIDOM M., *Phys. Rev. B*, **74** (2006) 134205.

[23] MOUNTAIN R. D. and BASU P. K., *J. Chem. Phys.*, **78** (1983) 7318.

[24] STEINHARDT P. J., NELSON D. R. and RONCHETTI M., *Phys. Rev. B*, **28** (1983) 784.

[25] TIAN Z. A., LIU R. S., PENG P., HOU Z. Y., LIU H. R., ZHENG C. X., DONG K. J. and YU A. B., *Phys. Lett. A*, **373** (2009) 1667.

[26] OSTWALD W., *Z. Phys. Chem.*, **22** (1897) 289.

[27] CHUNG S. Y., KIM Y. M., KIM J. and KIM Y. J., *Nat. Phys.*, **5** (2009) 68.

[28] ALEXANDER S. and MCTAGUE J., *Phys. Rev. Lett.*, **41** (1978) 702.

[29] SHEN Y. C. and OXTOBY D. W., *Phys. Rev. Lett.*, **77** (1996) 3585.

[30] FANG H. Z., HUI X., CHEN G. L. and LIU Z., *Phys. Lett. A*, **372** (2008) 831.

[31] DONG K. J., YANG R. Y., ZOU R. P., AN X. Z. and YU A. B., *EPL*, **86** (2009) 46003.